H_∞ Robust Control of a Seat Belt Load-limiting Device

Ke Dong, *Member, IEEE*

Abstract—**Continuously adaptive restraint system is currently the ideal state of restraint systems for occupant protection. It operates in real time during the impact according to the sensed operating conditions, such as seat belt force, occupant motion, crash severity, etc. In this paper, a linear time invariant (LTI) model of a crash dummy/vehicle system is built based on the method of system identification. The order of the system is first reduced using singular value decomposition (SVD). Next, a robust H_∞ controller is designed for the reduced-order system using linear matrix inequalities (LMIs). Simulations have been performed for the closed-loop system with both designed controller and the MADYMO occupant and vehicle model to demonstrate the performance of the designed controller.**

I. INTRODUCTION

Current occupant restraint systems for the frontal impact protection of a front seat passenger generally consist of a three-point seat belt, an airbag, and knee bolster. A restraint system design is regulated by the Federal Motor Vehicles Safety Standards (FMVSS), and also considers some highly publicized consumer metrics test requirements like the US New Car Assessment Program (USNCAP), as well as field performance. Adaptive restraint features, such as dual-stage airbag inflators and dual-stage seat belt load-limiters, have been implemented in order to meet these and other impact conditions. However, the potential benefits of this type of adaptive restraint systems are limited since their restraint settings are not continuously variable during crash, and since they usually require changing the restraint settings long before the impact happens.

In an effort to further improve the restraint performance under different crash conditions, real time control of the restraint systems has been studied and proposed in [1][2][3]. They showed that the real time control may improve the restraint performance during crash. In [1][2], a system identification method, which was proposed in [4][5], was used to obtain a low-order linear model, in which classic control design method based on gain margin and phase margin was used to design the LTI controller. In [6], a simplified multi-body mathematic model was built for the control purpose. Then a model predictive controller was designed for the linearized system. In [7] and [8], state estimator and reference governor were designed for real time restraint control. However, these previous researches focused mainly on the simplification of the restraint system model and the use of the classic control design method.

Ke Dong is with the General Motors Research & Development, Warren, MI 48090 USA (corresponding author , phone: 586-651-3027; fax: 586-986-0446; e-mail: ke.dong@gm.com).

In this paper, a model based robust control method based on linear matrix inequalities (LMIs) is developed and applied to the real time control design of a detailed occupant dynamics model with adaptive restraint system. To illustrate the method, a MADYMO/Matlab coupling model is built in the Matlab Simulink environment to control the chest deflection of a 50th percentile male Hybrid III dummy in a frontal rigid barrier impact with the impact speed of 35mph. Furthermore, both semi-active and full-active seat belt load-limiters have been studied in this paper. Saturation behavior of the load-limiter has also been considered.

II. SYSTEM MODELING AND IDENTIFICATION

MADYMO is a commercial software primarily used for crash dummy simulations. It provides a coupling functionality to allow the exchange of inputs and outputs with Matlab/Simulink in every time step [12].

A front passenger vehicle model with a dual stage airbag, a three point seat belt, a seat belt retractor load-limiter, a seat belt pre-tensioner, and knee bolster is built in MADYMO and correlated with the crash tests, as shown in Figure 1. A 50th %ile male Hybrid III dummy model was used in this study as an example. The method proposed in this paper can be generalized to apply for other vehicles and other dummy sizes. In the new USNCAP [10], the chest deflection of Hybrid III dummy is one of the injury indices in the overall star rating of the frontal impact. Since the seat belt force has direct impact on the chest deflection during the crash event, the seat belt retractor load-limiter is replaced by a continuously variable seat belt load-limiter, which uses smart materials such as Magneto rheological fluid and piezo stack to control the load limiting force [13], in this study as the primary adaptive restraint feature for controlling the chest deflection. There are two types of continuously variable seat belt load-limiters, which is under development of load-limiter suppliers. One is semi-active and the other is full active. The former only controls the resistant force required to release the seat belt and it does not generate force actively to pull the seat belt back into retractor. The latter provides both releasing and pulling forces. This paper considers both of them. The force controlled by the semi-active or full-active load-limiter is limited by the capability of the actuator. Therefore, saturation behavior is required to be considered in the modeling of the load-limiters.

The objective of this study is to design a tracking system for the chest deflection to track the reference signal by controlling the seat belt load-limiting force. By minimizing the reference signal, the chest deflection could be minimized as well if the tracking controller is designed properly. The closed-loop system is shown in

Figure 2, in which $\tilde{P}$ is the vehicle and occupant system, $\tilde{K}$ is the controller to be designed, $\tilde{r}_{cd}(t)$ is the reference signal for the chest deflection, $\tilde{y}_{cd}(t)$ is the measurement of the chest deflection from MADYMO model, $\tilde{F}(t)$ is the seat belt load limiting force, and $\ddot{x}_v(t)$ is the vehicle deceleration pulse.
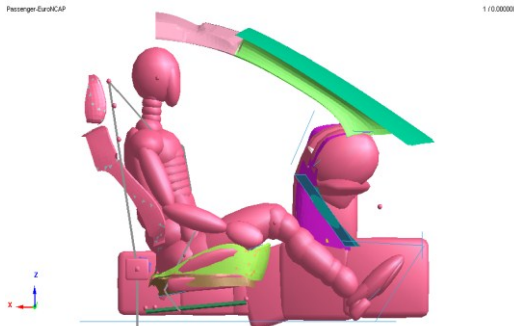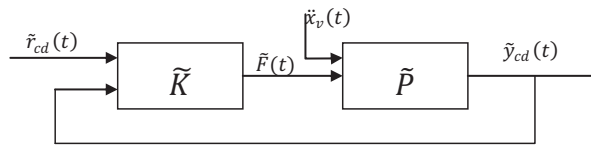

Figure 1, MADYMO Vehicle/Occupant Model


Figure 2, Nonlinear closed-loop System

Seat belt load-limiting force $\tilde{F}(t)$ is different from the force on the seat belt $F_s(t)$. The semi-active seat belt force actuator in $\tilde{P}$ is modeled as a braking unit with friction coefficient $\mu_s(t) = 0.3$. $\tilde{F}(t)$ is the brake force. There is also a saturation of the seat belt actuator, which limits the maximum force to be 50kN. The relationship between $F_s(t)$ and $\tilde{F}(t)$ is defined below

$$F_s(t) = \begin{cases} F_s(t) & for\ F_s(t) < \mu_s\tilde{F}(t) \\ \mu_s\tilde{F}(t) & for\ \mu_s\tilde{F}(t) < F_s(t) < 50\mu_s kN \\ 50\mu_s kN & for\ F_s(t) > 50\mu_s kN \end{cases} \quad (1)$$

Because of the complexity of $\tilde{P}$, a system identification method is used to estimate the linear model using measurements on $\tilde{P}$. The baseline model is chosen as the operating point. The seat belt load limiting force of the baseline model is set as $F_0(t) = 1.5$kN. Due to friction force on D-ring, the shoulder belt force is about 2kN. Then baseline shoulder belt force $F_{s0}(t)$ and chest deflection $y_{cd0}(t)$ are shown in Figure 3.

The linear system around the operating point is identified by adding perturbation $\delta F(t)$ to $F_0(t)$ and measuring the perturbed output $\delta y_{cd}(t)$. By simulating the baseline model, the occupant contacts airbag at 48ms. Two time instants $\tau_1 = 45$ ms and $\tau_2 = 50$ ms have been chosen for adding the perturbation. Four amplitudes of the step perturbation $\epsilon(t - \tau)$ are chosen, $\delta F_1(t) = 50$ N, $\delta F_2(t) = 100$ N, $\delta F_3(t) = 150$ N and $\delta F_4(t) = 200$ N. Four experiments are performed for each time instant with the open loop system P. The perturbed output $y_{cd}(t) = y_{cd0}(t) + \delta y_{cd}(t)$ is measured with the perturbed input $F(t) = F_0(t) + \delta F \cdot \epsilon(t - \tau)$. The

normalized responses $\frac{\delta y_{cd}}{\delta F}$ are derived for both time instants, which are shown in Figure 4 with the average of all eight experiments.
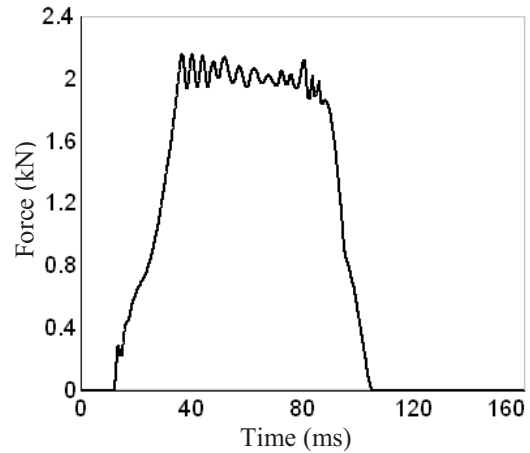
(a) Shoulder Belt Force
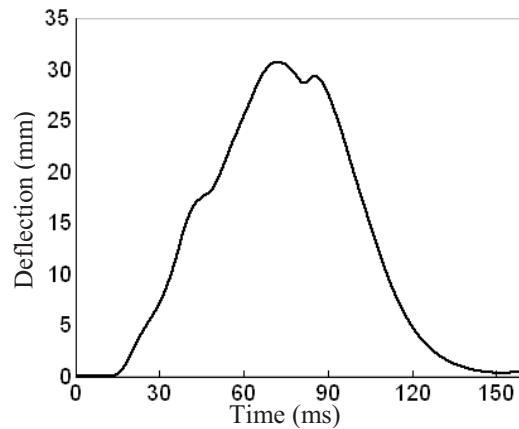
(b) Chest Deflection
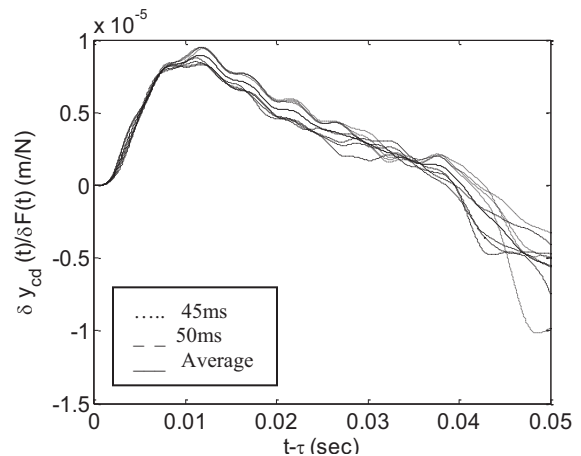Figure 3, Seat belt load-limiter function profiles

Figure 4, Normalized responses of chest deflection

There is consistent difference between the normalized responses of $\tau_1 = 45$ ms and $\tau_2 = 50$ ms after $t - \tau > 13$ms.p The difference of the steady state response is caused by the different airbag pressure. The transient response of $t - \tau < 13$ ms well represents the relationship between

$\delta F(t)$ and $\delta y_{cd}(t)$. The designed robust controller will be able to tolerate the disturbance caused by airbag and other factors. By using the method of Hankel matrix and choosing the four largest singular values [4][5], a fourth order discrete time model can be derived from the normalized responses. The obtained discrete time model is transformed to continuous time domain by zero order hold conversion. A fourth order linear time invariant model P is generated for $\tilde{P}$. The model P is represented in state space form as

$$\begin{bmatrix} \dot{x}(t) \\ y(t) \end{bmatrix} = \begin{bmatrix} A & B \\ C & D \end{bmatrix} \begin{bmatrix} x(t) \\ u(t) \end{bmatrix} \qquad (2)$$

where $x, \dot{x} \in \mathbb{R}^4, y, u \in \mathbb{R}^1$,

$$A = \begin{bmatrix} -15.31 & 3.968 & -84.65 & 37.19 \\ 241.3 & -31.71 & 133.5 & -41.09 \\ 301.2 & -284.9 & -121 & 53.96 \\ -183.4 & 75.99 & 231.2 & -108.2 \end{bmatrix}, B = \begin{bmatrix} -0.1458 \\ 0.3588 \\ 0.7102 \\ -0.3619 \end{bmatrix}, C = [-2.86 \quad 1.949 \quad -1.578 \quad 0.859] \times$$

$10^{-3}, D = 0$, u is the control input of seat belt load-limiting force, y is the controlled output of the chest deflection.

The bode diagram of P are plotted in Figure 5. The open loop system is unstable as shown.
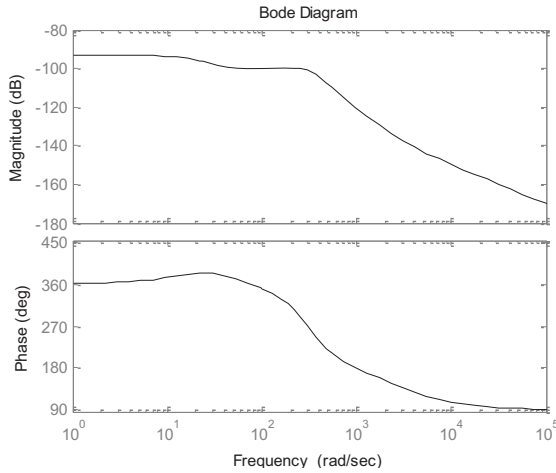

Figure 5, Bode diagram of P

III. $\boldsymbol{H}_\infty$ ROBUST CONTROL DESIGN

H_∞ control is a mature method for LTI system to guarantee stability and minimize the gain from disturbance input to error output. Consider a proper continuous time LTI plant P in state space form

$$\begin{bmatrix} \dot{x}(t) \\ e(t) \\ y(t) \end{bmatrix} = \begin{bmatrix} A & B_1 & B_2 \\ C_1 & D_{11} & D_{12} \\ C_2 & D_{21} & D_{22} \end{bmatrix} \begin{bmatrix} x(t) \\ d(t) \\ u(t) \end{bmatrix} \qquad (3)$$

The suboptimal H_∞ control problem can be formulated as finding a controller K in the form of

$$\begin{bmatrix} \dot{x}_k(t) \\ u_k(t) \end{bmatrix} = \begin{bmatrix} A_K & B_K \\ C_K & D_K \end{bmatrix} \begin{bmatrix} x_K(t) \\ y_K(t) \end{bmatrix} \qquad (4)$$

such that
1) The closed-loop system is internally stable.
2) The H_∞ norm of $\mathcal{F}(P, K)$ is strictly less than γ.

The output feedback controller synthesis condition has been formulated as LMIs in [14].

Lemma 1 - Given an open loop LTI system P in (3), the continuous time γ suboptimal H_∞ problem is solvable if and only if there exist positive definite matrices $R \in \mathbb{S}_+^{n \times n}$ and $S \in \mathbb{S}_+^{n \times n}$ satisfying

$$\begin{bmatrix} \mathcal{N}_R & 0 \\ 0 & I \end{bmatrix}^T \begin{bmatrix} AR + RA^T & RC_1^T & B_1 \\ C_1 R & -\gamma I & D_{11} \\ B_1^T & D_{11}^T & -\gamma I \end{bmatrix} \begin{bmatrix} \mathcal{N}_R & 0 \\ 0 & I \end{bmatrix} < 0 \quad (5)$$

$$\begin{bmatrix} \mathcal{N}_S & 0 \\ 0 & I \end{bmatrix}^T \begin{bmatrix} A^T S + SA & SB_1 & C_1^T \\ B_1^T S & -\gamma I & D_{11}^T \\ C_1 & D_{11} & -\gamma I \end{bmatrix} \begin{bmatrix} \mathcal{N}_S & 0 \\ 0 & I \end{bmatrix} < 0 \quad (6)$$

$$\begin{bmatrix} R & I \\ I & S \end{bmatrix} \geq 0 \qquad (7)$$

Where
$\mathcal{N}_R = \ker[B_2^T \quad D_{12}^T]$ and $\mathcal{N}_S = \ker[C_2 \quad D_{21}]$.

After solving the positive definite matrices R and S, the H_∞ controller can be constructed through the following scheme [15][16]:
(i) Let matrices $M \in \mathbf{R}^{n \times n}$, $N \in \mathbf{R}^{n \times n}$ and $MN^T = I - RS$ and define
$$F = -(D_{12}^T D_{12})^{-1}(\gamma B_2^T R^{-1} + D_{12}^T C_1)$$
$$L = -(\gamma S^{-1} C_2^T + B_1 D_{21}^T)(D_{21} D_{21}^T)^{-1}$$
(ii) Construct the state-space matrices of one nth-order, strictly proper controller as
$$A_K = -N^{-1}[A^T + S(A + B_2 F + LC_2)R$$
$$+ \gamma^{-1} S(B_1 + LD_{21})B_1^T$$
$$+ \gamma^{-1} C_1^T (C_1 + D_{12}F)R]M^{-T}$$
$$B_K = N^{-1}SL$$
$$C_K = FRM^{-1}$$
$$D_K = 0$$

By adding a weighting function W_e to the error output $e(t) = r_{cd}(t) - y_{cd}(t)$, the plant is reconstructed as shown in Figure 6.

The weighting function $W_e(s)$ is usually selected to be like a low-pass filter in the form of

$$W_e(s) = \lambda \frac{s + \rho_1^\mu}{s + \tau_1}, \qquad \mu \in \{0,1\} \qquad (8)$$

which has larger weighting in low frequency and smaller weighting in high frequency. μ is set to one in order to consider both low-frequency and high-frequency disturbance. The formula $W_e(\infty) = \lambda$ represents the weighting factor for the disturbance rejection ability at high frequency. By increasing λ, the high-frequency disturbance will be rejected more. The formula $W_e(0) = \frac{\lambda \rho_1}{\tau_1}$ represents the weighting

factor for the steady-state error. By increasing ρ_1, the steady-state error will decrease. However, there is no general formula available to express the dependence between the overshoot/rise time and the frequency response of the weighting function $W_e(s)$. Based on the previous researches on weighting function [17], the response time is roughly inversely proportional to the bandwidth, and the overshoot depends on the peak magnitude and the roll-off rate of the frequency response. By increasing ρ_1, the bandwidth can be widened. It is desired to have a peak overshoot less than 20% and settling time less than 10ms. The design goal can be achieved by choosing the weighting function as

$$W_e = 0.5\frac{s + 8000}{s + 4} \qquad (9)$$

Then the output response $y_{cd}(t)$ could have a small steady state error of 0.1% with relatively fast transient response. The frequency response of W_e is shown in Figure 7.
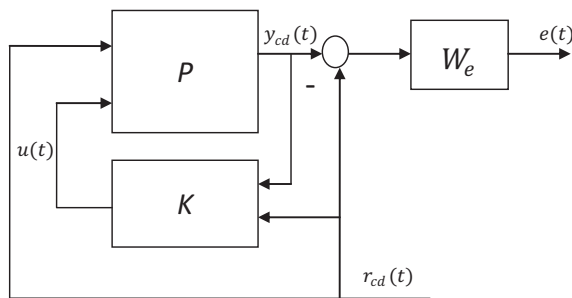

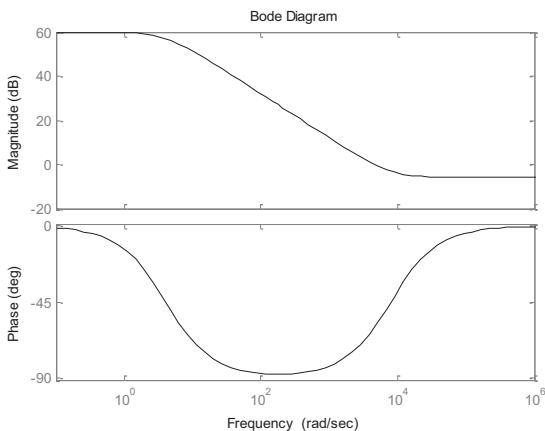Figure 6, Re-constructed system with weighting function

Figure 7, Frequency response of $\mathbf{W_e}$

By solving LMIs in Equations (5) - (7), a fifth order LTI controller with two inputs and one output is obtained. The closed loop system $\mathcal{F}(P, K)$ has the H_∞ norm of $\gamma = 9.1108$. The step response of the closed loop system $\mathcal{F}(P, K)$ is shown in Figure 8.

Since the controller design is based on linear approximation of the system at the equilibrium point of 1.5kN seat belt load-limiting force, in order to simulate the performance of the original nonlinear system, the linear controller has to be added to the equilibrium point. Then the system structure becomes as shown in Figure 9.
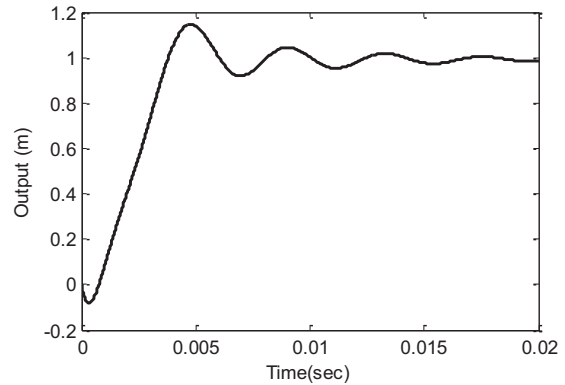
(a) Chest Deflection
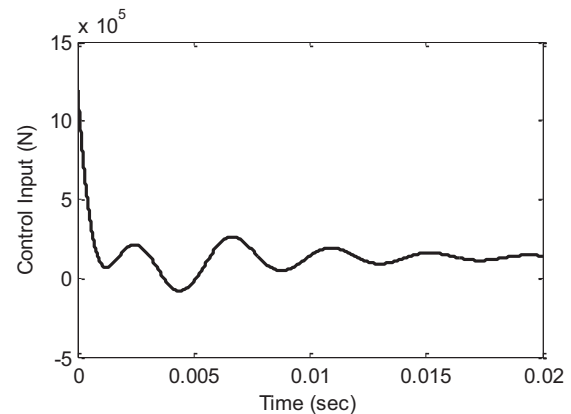
(b) Seat Belt Force

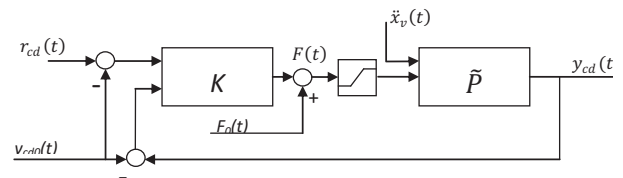Figure 8, Step response of $\mathcal{F}(\mathbf{P}, \mathbf{K})$

Figure 9, Nonlinear occupant/vehicle model with the linear controller

IV. SIMULATION RESULTS OF SEMI-ACTIVE LOAD-LIMITER

Two reference signals of $r_{cd}(t)$ are simulated with the design the controller and nonlinear MADYMO occupant/vehicle model. In the first simulation, the reference chest deflection is set to 28mm. Figure 10 shows the simulation results. Figure 10 (a) shows the time history of chest deflection. The chest deflection is maintained at 28mm level as long as possible. Figure 10 (b) shows the shoulder belt force versus seat belt payout. Initially, the load-limiter has a high limiting force to hold the seat belt until the chest deflection reaches the desired value of 28mm. Then the real-time controller starts reducing the seat belt limiting force to maintain the constant chest deflection. At the end of the crash, the crash deceleration is reduced to zero. The load-limiter still tries to track the reference chest deflection.

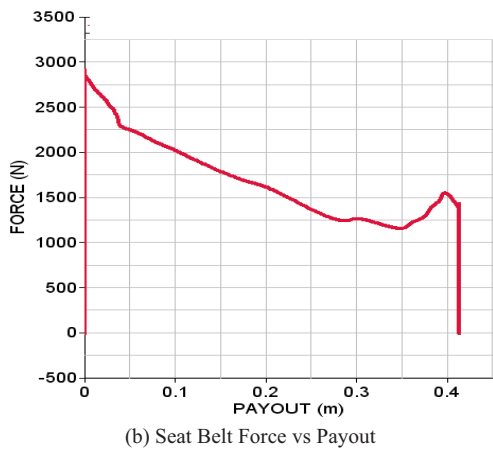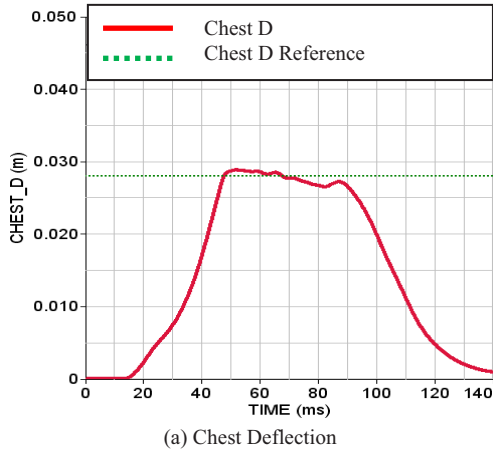So it holds the seat belt again to generate more seat belt force to compensate the reduced deceleration.

(a) Chest Deflection

(b) Seat Belt Force vs Payout

Figure 10, Simulation results of 28mm chest deflection reference

away from the original equilibrium point of 30mm chest deflection as shown in Figure 3.

(a) Chest Deflection

(b) Seat Belt Force vs Payout
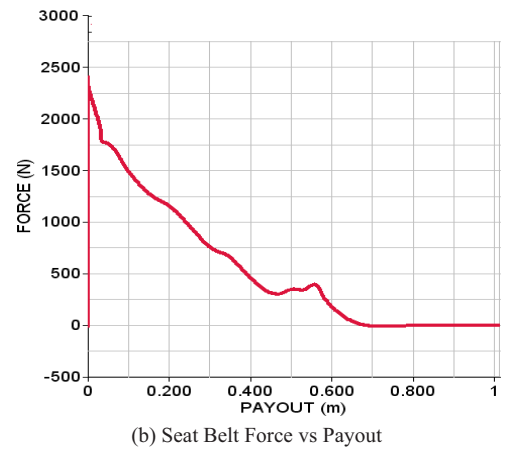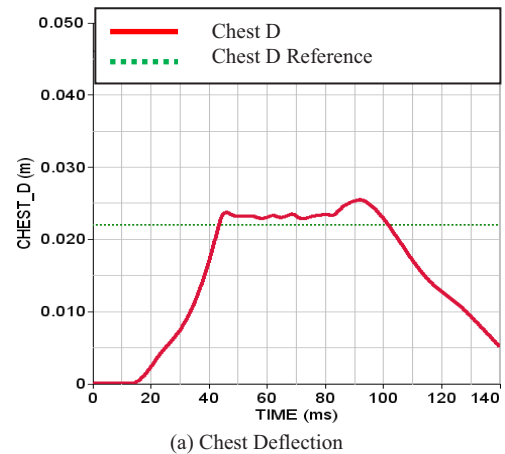
Figure 11, Simulation results of 22mm chest deflection reference

In the second simulation, the desired chest deflection is set to 22mm. All the other settings are the same as the previous simulation. The real-time controller tries to control the load-limiter to maintain the chest deflection at 22mm and outputs a lower seat belt limiting force to achieve that low chest deflection. The lower seat belt force causes more forward movement of the upper body. However, the setting of the airbag vent and inflator has not been changed. Eventually, the airbag are compressed hard at 90ms, which causes a bump in the chest deflection. At this time, however, the controller already reduced the seat belt force to almost zero.

Choosing an appropriate chest deflection reference is important to achieve the optimal tracking performance. Chest deflection at the original equilibrium point can be a starting point. By trying to reduce chest deflection from equilibrium point, the optimal chest deflection reference usually can be achieved within several iterations.

It is not necessary to achieve a lower chest deflection by reducing the reference value because there are other factors, such as airbag, acting on the chest load. From the two simulation results which vary the reference command from 28mm to 22mm, the designed H_∞ controller is able to provide very good robustness even the operating point moves far
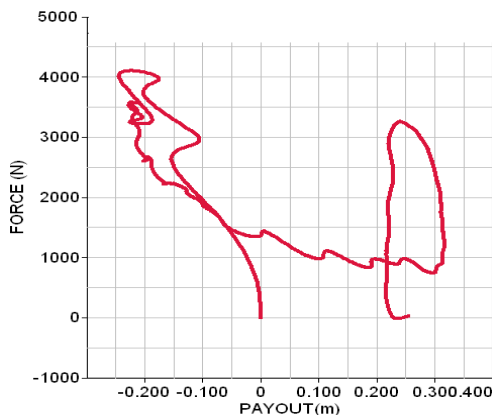
V. SIMULATION RESULTS OF ACTIVE LOAD LIMITER

In the previous sections, the seat belt load-limiting actuator is modeled as a semi-active device, which is based on friction. So the actuator only controls the resistant force when the seat belt is pulling out. The semi-active actuator is unable to generate extra force to pull the seat belt back into retractor, which means the actuation force on the seat belt will never exceed the belt force generated by the occupant deceleration. However, a full active load-limiting actuator is able to fully control the seat belt force by either pulling or releasing the seat belt. This kind of active device may provide additional benefit to the real time control of the adaptive restraint systems.

The same approach discussed in previous sections is applied to the system with active load-limiter including SVD based system identification and LMI based H_∞ control design. Figure 12 shows the simulation results of the closed loop system with full-active load-limiter.
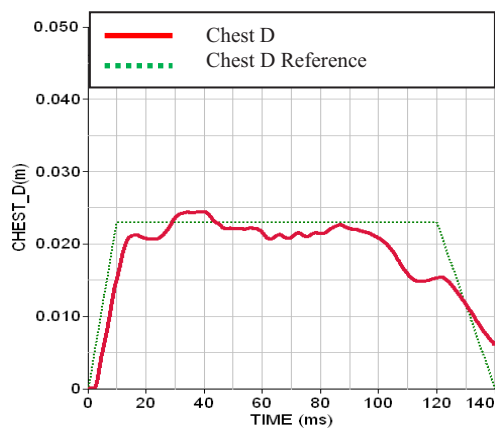
(a) Chest Deflection

(b) Seat Belt Force vs Payout

Figure 12, Simulation results of active load-limiter

By simulating the closed-loop system with the crash dummy/vehicle model and the linear H_∞ robust controller, the designed controller meets the desired chest deflection performance criteria. Although the saturation has been introduced into the actuator and the reference signal of chest deflection varies from 28mm to 22mm, the controller still stabilizes the nonlinear system with good robustness.

In order to apply the proposed method to an occupant during crash, real-time measurement of occupant's chest deflection is necessary, which is not possible with current technology. A surrogate measurement, such as seat belt force or airbag pressure, may be used to indirectly estimate the chest deflection. Further development to address this limitation is necessary before implementing this real time control method in a production vehicle.

As shown in Figure 12 (a), the reference signal is selected to be a ladder-shaped curve in order to avoid high actuating force at the beginning of the simulation. The system is unable to track the reference well after 100ms because the occupant lacks the forward movement caused by vehicle deceleration by that time. In Figure 12 (b), the seat belt force versus payout is shown. The active actuator, which has maximum actuating force of 6kN, applies large pulling force up to 4kN to the occupant to tighten the seat belt. Then gradually reduces the actuating force to compensate the extra force caused by vehicle deceleration. At the end, the actuating force increases again because the vehicle deceleration reduces. Comparing to the semi-active load-limiter, the active load-limiter is able to further reduce the chest deflection by fully controlling the seat belt force.

VI. CONCLUSION

A real time control for a nonlinear crash dummy/vehicle system has been developed to control the chest deflection of the crash dummy by controlling the seat belt force in real time during a crash. The nonlinear crash dummy/vehicle system is first approximated to a fourth order linear system by a system identification method based on singular value decomposition. Then, the LMI based H_∞ control theory is applied to the approximated linear system to obtain a robust controller.

REFERENCES

[1] Hesseling, R. J., "Identification and Control for Future Restraint Systems", Proc. Of the 42nd IEEE Conference on Decision and Control, pp. 2780-2785, 2003

[2] Hesseling, R. J., "Active Restraint Systems - Feedback Control of Occupant Motion", Ph. D. Thesis, Technische Universiteit Eindhoven, 2004

[3] Griotto, G., Lemmen, P. and van den Eijnden, E, etc. "Real Time Control of Restraint Systems in Frontal Crashes", SAE 2007-01-1504, 2007

[4] Kung, S. Y., "A New Identification and Model Reduction Algorithm via Singular Value Decomposition," in Proc. of the 12th Asilomar Conf. on Circuits, Systems and Computers, California, USA, pp. 705-714, 1978

[5] van Helmont, J. B., van der Weiden, J. J., and Anneveld, H., "Design of Optimal Controllers for a Coal Fired Benson Boiler based on a Modified Approximate Realization Algorithm," in Proc. Of Application of Multivariable System Techniques. London, UK, pp. 313-320, 1990

[6] van der Laan, E.P., Veldpaus, F.E., de Jager, B., and Steinbuch, M., "Control Oriented Modeling of Occupants in Frontal Impacts," International Journal of Crashworthiness, 14(4), p. 323–337. 2009

[7] van der Laan, E.P., Veldpaus, F.E., and Steinbuch, M. "State Estimator Design for Realtime Controlled Restraint Systems," In Proceedings of the American Control Conference (ACC), 11-13 Jul, New York City, NY, USA, p. 242–247. 2007

[8] van der Laan, E.P., Luijten, H.J.C., Veldpaus, F.E., Heemels, W.P.M.H., and Steinbuch, M. "Reference Governors for Controlled Belt Restraint Systems," In Proc. of the International Conference on Vehicular Electronics and Safety (ICVES), 22-24 Sep, Columbus, OH, USA, p. 114–119. 2008

[9] National Highway Traffic Safety Administration (NHTSA), "Federal Motor Vehicle Safety Standard no. 208; Occupant crash protection," U.S. Department of Transportation, Tech. Rep. 49 CFR 571.208, 2004

[10] -, "U.S. New Car Assessment Program", http://www.safecar.gov

[11] National Highway Traffic Safety Administration (NHTSA), "Consumer Information; New Car Assessment Program" U.S. Department of Transportation, Docket No. NHTSA-2006-26555, 2006

[12] MADYMO User Manual, v 7.1, TNO, December 2010

[13] Anders, L., Andes, L. I., Anders, I., "Seat Belt Arrangement", U.S. Patent US7478836, 2009

[14] Gahinet, P., Apkarian, P., " A Linear Matrix Inequality Approach to H_∞ Control", International Journal of Robust and Nonlinear Control, 4 (4), p. 421-448, 1994

[15] Wu, F., "A Generalized LPV System Analysis and Control Synthesis Framework," International Journal of Control, 74 (7), p. 745-759, 2001

[16] Zhou, K., Doyle, J.C., and Glover, K. (1996). Robust and Optimal Control. Prentice-Hall, Upper Saddle River, NJ, USA.

[17] Hu, J., Bohn, C., Wu, H.R., "Systematic H_∞ Weighting Function Selection and its Application to the Real-time Control of a Vertical Take-off Aircraft," Control Engineering Practice, 8 (2000), p. 241-252, 2000